

Beniwal, A., Ganguly, P., Gond, R., Rawat, B. and Li, C. (2023) Room temperature operated PEDOT: PSS based flexible and disposable NO₂ gas sensor. *IEEE Sensors Letters*, 7(9), 2001804. (doi: [10.1109/lsens.2023.3308518](https://doi.org/10.1109/lsens.2023.3308518))



Copyright © 2023 IEEE. Reproduced under a [Creative Commons Attribution 4.0 International License](https://creativecommons.org/licenses/by/4.0/).

For the purpose of open access, the author(s) has applied a Creative Commons Attribution license to any Accepted Manuscript version arising.

<https://eprints.gla.ac.uk/305332/>

Deposited on: 23 August 2023

Room Temperature Operated PEDOT:PSS based Flexible and Disposable NO₂ Gas Sensor

Ajay Beniwal¹, Priyanka Ganguly², Rahul Gond³, Brajesh Rawat³ and Chong Li¹

¹Electronics and Nanoscale Engineering, James Watt School of Engineering, University of Glasgow, G12 8QQ, Glasgow, UK

²School of Human Sciences, London Metropolitan University, N7 8DB, UK

³Department Electrical Engineering, Indian Institute of Technology Ropar, Rupnagar, Punjab, 140001, India

Received 1 Nov 2016, revised 25 Nov 2016, accepted 30 Nov 2016, published 5 Dec 2016, current version 15 Dec 2016. (Dates will be inserted by IEEE; "published" is the date the accepted preprint is posted on IEEE Xplore®; "current version" is the date the typeset version is posted on Xplore®).

Abstract— This work presents a flexible and disposable nitrogen dioxide (NO₂) gas sensor based on Poly(3,4-ethylenedioxythiophene):poly(styrenesulfonate) (PEDOT:PSS), operating at room temperature (RT). The gas sensing layer, composed of PEDOT:PSS, is deposited on interdigitated electrodes (IDEs) made from graphene-carbon ink, which are screen printed onto a paper substrate using the drop casting method. The FTIR and SEM analysis are carried out to understand the successful deposition and surface morphology analysis of the sensing layer. The NO₂ sensing properties are explored in the range 0.5 ppm to 50 ppm at room temperature (27 °C ± 2 °C). The sensor displays significant % response viz. 0.79 % to 12.97 % in the measured range 0.5 ppm to 50 ppm. Other important sensing characteristics like response and recovery times (210 s / 60 s at 0.5 ppm), repeatability, reproducibility along with sensing mechanism are also presented. The findings of this study suggest that the developed sensor holds promise for various application areas.

Index Terms— Disposable NO₂ sensor; eco-friendly; flexible electronics; gas sensing; PEDOT:PSS.

I. INTRODUCTION

Nitrogen dioxide (NO₂) is one of the toxic and harmful gas, commonly released from burning of fossil fuels, vehicles, and automotive industries [1, 2]. It is also considered as a main air pollutant, which contributes to acid rain formation, photochemical smog and detrimental to human health [3]. Along with this, exhaled nitric oxide (NO; NO is oxidized to NO₂) is considered as a potential biomarker for detection of lung diseases including asthma [4]. Therefore, its detection is vital for healthcare sector as well. Further, prolonged exposure to NO₂ can cause mild irritation to nose, eyes, nose, and throat, and can leads to respiratory failure and even causes death [2, 5]. Therefore, it is of utmost importance to develop a high performance, user-friendly, cost effective and portable NO₂ sensor for its possible applicability to diverse application areas including healthcare, environmental monitoring, automotive industry etc. Although a wide variety of sensors/materials including metal oxides, 2D material and conducting polymers have been reported for NO₂ detection operating at different conditions [1, 5-11]. Most of these sensors are using non eco-friendly sensing materials and/or, substrates and/or, electrodes contributing towards growing electronic waste issue [12]. Therefore, there is necessity to come up with environmentally friendly sensing solutions by developing a disposable sensor for NO₂ detection along with other important features like good sensing performance, facile, economical, resource-efficient, and flexible sensor.

In this work, we demonstrate a RT operated NO₂ sensor using PEDOT:PSS sensing layer drop casted on graphene-carbon IDEs printed on a paper substrate. The choice of gas sensing material is due to its environment-friendly and biocompatible nature, good thermal stability, easy processing, and compatibility towards solution-based processes [13, 14]. Further, choice of paper as a substrate is due to its disposability, recyclability, and widespread availability. The NO₂ sensing properties are investigated in the range 0.5-50 ppm at RT and the sensor exhibited significant sensing performance. The results indicate that the developed sensor hold promise for numerous

application areas, like healthcare, environmental monitoring, and automotive industry.

This paper is organised as follows: Section II presents the details of the materials used, sensor fabrication process and gas sensing set-up. The material characterisation and gas sensing results are discussed in Section III and conclusions are described in Section IV.

II. MATERIALS AND METHODS

A. Materials and Sensor Fabrication

Graphene-carbon ink (C2171023D1: Graphene Carbon Ink:BG04, Sun Chemical), PEDOT:PSS (PH 1000, Ossila) and paper/substrate (matt double sided photopaper) were used for sensor development. The IDEs were printed using Screen Stencil Printer C920 from AUREL Automation. The complete fabrication and modification using PEDOT:PSS were done based on our previous work [15].

B. Gas Sensing Set-up and Sensor Characterisations

The fabricated sensor was characterised using Fourier-transform infrared spectroscopy (FTIR) and scanning electron microscopy

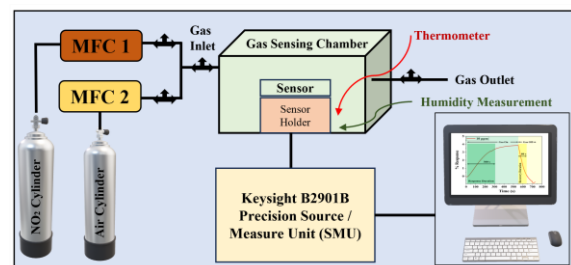


Fig. 1 Schematic illustration of gas sensing set-up.

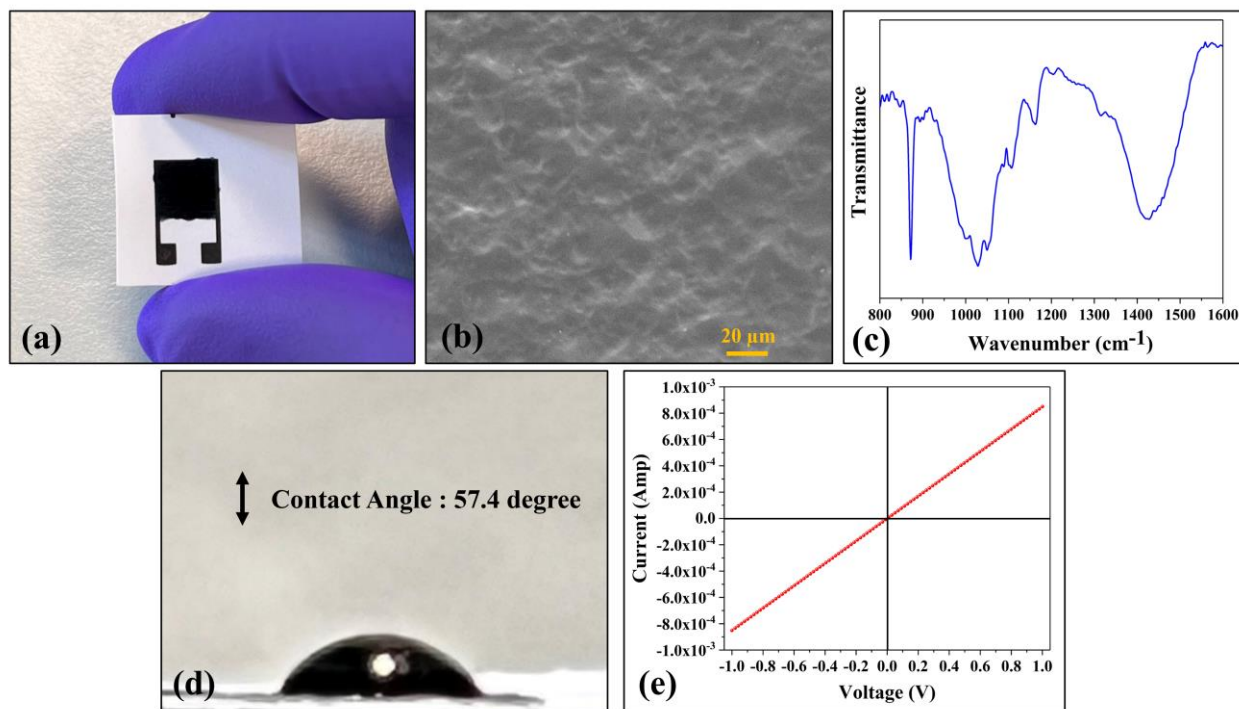


Fig. 2 (a) PEDOT:PSS based sensor developed on graphene-carbon interdigitated electrodes screen-printed on paper substrate. (b) SEM image of the PEDOT:PSS based sensing layer at 20 μm scale. (c) FTIR analysis of the developed sensor. (d) Contact angle measurement of the sensing layer. (e) I-V characterization of the developed sensor.

(SEM). For device characterisation, a controlled environment gas sensing chamber equipped with a sample holder was utilized (as shown in Fig. 1). The current-voltage (I-V) characteristics were recorded using a Keysight B2901B source meter. All gas sensing measurements were conducted within the closed controlled environmental chamber, at RT and humidity conditions below 5% relative humidity.

III. RESULTS AND DISCUSSION

A. Material Characterisation

The PEDOT:PSS-based sensor, which was developed on screen printed graphene-carbon interdigitated electrodes is shown in Fig. 2(a). To examine the surface morphological characteristics of the sensing layer, SEM analysis was employed. The SEM image of the sensing layer, at a scale of 20 μm , as shown in Fig. 2(b), reveals a rough surface morphology of the drop-casted PEDOT:PSS layer, which could be advantageous for room temperature operation. Furthermore, the deposited sensing layer on IDEs was subjected to FTIR analysis and the results are illustrated in Fig. 2(c). The infrared spectra display all the notable peaks in PEDOT:PSS and confirm the successful deposition of the sensing layer. The peak at 1340 cm^{-1} is attributed to C=O stretching and similarly other peaks at 1180 cm^{-1} , 1120 cm^{-1} and 1040 cm^{-1} can be attributed to C-O-C bond vibrations. Moreover, the major stretching around 1120 cm^{-1} , and 860 cm^{-1} are the bands linked with the sulfur bonds (C-S) of the thiophene ring in the PEDOT:PSS. For instance, the peaks for the sulfonic acid group (S=O) of the PSS chain are observed near 1400 cm^{-1} and the O-S-O signal at 1010 cm^{-1} [16, 17].

The hydrophilic nature of the sensing surface was evaluated using the sessile drop method for contact angle measurement. This analysis provides insights into the impact of humidity interference on the gas sensing characteristics, as PEDOT:PSS based sensor developed using the same route has already been investigated for the humidity sensing purpose in our previous work [15]. The contact angle measured for the

droplet on the sensing layer surface is around 57.4° (Fig 2 (d)). Contact angle being lower than $< 90^\circ$ shows the hydrophilic nature of the surface. Lesser the value of the angle to 90° , higher is the hydrophilicity. In this case, the sensor surface shows a moderate hydrophilicity of the sensing layer. Fig. 2(e) shows the excellent I-V characteristics of the sensor displaying a linear line crossing through the origin. Thus, indicating the formation of a good ohmic contact [18].

B. Sensing Analysis

The chemiresistive sensing behaviour of the fabricated sensor is examined towards NO_2 gas. The sensing characteristics were evaluated within the sensing range of 0.5 ppm to 50 ppm, at room temperature operating conditions. The change in resistance behaviour of the sensor towards NO_2 detection is represented in the form of % response vs time graph in Fig. 3(a). The % response is mathematically defined as $(\Delta R * 100) / R_b$, where ΔR is calculated as $R_g - R_b$; R_g is the resistance of the sensor in the presence of target gas and R_b is the baseline resistance. The sensor exhibited distinguishable response even at extremely low concentration viz. 0.5 ppm of NO_2 . The sensor is approved to appropriately work at room temperature (without any heating element), which is advantageous from power consumption perspective along with eliminating the need of additional complex circuitry. Room temperature operated sensors are also a great fit and highly desirable in explosive/flammable environments and portable sensing systems. Subsequently, the individual response (as shown in Fig. 3a) at each concentration i.e., 0.5 ppm, 1 ppm, 10 ppm and 50 ppm are further examined. The % response vs concentration graph is shown in the Fig. 3(b). The obtained results indicate % responses of around 0.79 %, 1.14 %, 3.86 % and 12.97 % for NO_2 gas with concentration of around 0.5 ppm, 1 ppm, 10 ppm and 50 ppm, respectively. The gas sensing response depicts a nearly linear behaviour having a linear fit Adj. R-Square of 0.99495.

Fig. 3(c) illustrates the response and recovery times of the sensor at 10 ppm NO_2 concentrations. The response time is analysed as the time taken by the sensor to reach 90% of the stable % response value, while the recovery time is returning to its initial value after removing

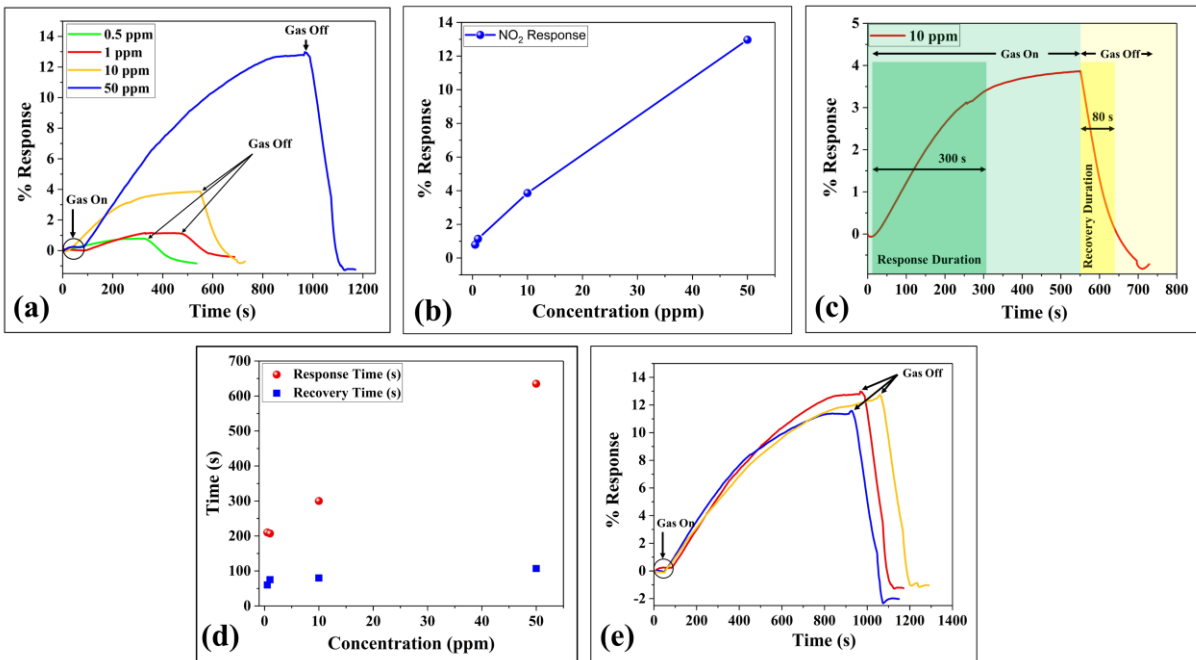


Fig. 3. NO₂ sensing properties of PEDOT:PSS based sensor in concentration range 0.5 ppm to 50 ppm: (a) Response vs time graph with gas on/off cycles. (b) % Response vs concentration graph. (c) Response and recovery time analysis at 10 ppm of NO₂ concentration. (d) Response and recovery times for 0.5-50 ppm. (e) Cyclic repeatability analysis.

the target gas and reaching 10%. The response and recovery times are observed as 300 sec and 80 sec, respectively as shown in Fig. 3(c). Further, Fig. 3(d) shows that the response/recovery times are found to be approximately 210 s / 60 s, 207 s / 75 s, and 635 s / 107 s, for 0.5 ppm, 1 ppm, and 50 ppm, respectively. The response and recovery times are slightly sluggish which may be due to RT operation of the sensor. Furthermore, we also investigated the repeatability of the sensing characteristics towards NO₂ detection at 50 ppm. The measurement results as shown in the Fig. 3(e), indicate that the sensor has repeatable sensing characteristics. However, post analysing the repeatability of the sensor at 50 ppm, when the sensor is exposed to a higher concentration, there is no significant change in the sensing response is obtained. This could be ascribed either to saturation of the sensing layer or due to blocked adsorption sites on the sensing surface. Moreover, the reproducibility analysis is also carried out by fabricating the replica sensor and comparing the NO₂ sensing performance (at 0.5 ppm) with the original sensor. The % response for replica sensor is observed as 0.845 %, which is comparable with the original sensor response i.e., 0.79 % at 0.5 ppm. The marginal error is observed as

6.96%. The obtained results suggest sensor's reproducible performance towards NO₂ detection. The experimental results indicate sensor's suitability for multiple application areas viz. healthcare, environmental and industrial sectors.

Table 1 benchmarks our developed sensor with the literature studies based on pristine or doped/composite of PEDOT:PSS. The comparative analysis clearly shows that our work provides merits over the background reports considering disposability and flexibility as a viable option along with the reasonable NO₂ sensing performance.

C. Sensing Mechanism

The fabricated sensor coated with a PEDOT:PSS film shows effective detectability of NO₂. The sensing mechanism could be ascribed as: PEDOT:PSS based sensing layer provides enough surface area and active sites for the gas molecules to interact and physisorbed on the surface. The FTIR spectra displayed the different functional groups present and validating the influence of the active sites present on the surface of the sensor.

Table 1: Performance benchmarking of our developed sensor with existing PEDOT:PSS based NO₂ sensors

Material Composition	Fabrication Route	Operating Temp	Sensing Range	Disposability	Substrate	Flexibility	Ref.
Doped PEDOT:PSS	Ink-jet printing	RT	10 ppm	No	Silicon	No	9
PEDOT-PSS/TiO ₂ nanofibres	Electrospinning technology	RT	10 - 130 ppb	No	Silicon	No	10
GO-PEDOT:PSS nanocomposite	Drop casted	RT	5 - 100 ppm	No	Langasite (LGS)	No	5
WO ₃ -PEDOT:PSS nanocomposites	Gravure-printed	RT	50 - 200 ppb	No	Polyimide	Yes	1
PEDOT:PSS/ Ti ₃ C ₂ T _x (MXene)/ZnO composites	spin-coating and drop casting	RT	400 - 1000 ppb	No	Al ₂ O ₃ Ceramic	No	11
PEDOT:PSS on printed graphene-carbon IDEs	Screen Printing and Drop Casting	RT	0.5 - 50 ppm	Yes	Paper	Yes	This Work

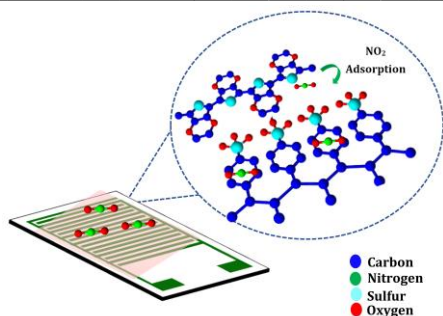


Fig. 4 Schematic illustration of sensing mechanism.

In addition, the resistance of the sensor increased with the increase in concentration of the gas and the resistance lowered to its baseline when dry air was flushed into the system. The role of PEDOT:PSS in the sensing process can be explained through several plausible explanations [5, 19-21]. One explanation is the direct charge transfer between the NO_2 gas molecules and the sensing surface of the sensor. The PEDOT:PSS surface adsorbs NO_2 gas molecules, resulting in the transfer of charges between the conductive film and NO_2 gas molecules. The π electrons present in the sensing film (PEDOT:PSS) alter the charge transfer occurred by NO_2 molecules. This causes the formation of the neutral backbone of the polymeric chain by the reduced amount of charge carriers which subsequently leads to the reduction in the electrical conductivity.

Another plausible explanation of the increase in the resistance measured could be the diffusion of the gas molecules within the polymer matrix. The PEDOT:PSS film has an interesting structure, with each PSS chain electrostatically interacting with several shorter PEDOT chains. The shorter distance between the chain molecules promotes charge carriers hopping between the PEDOT chains. The physisorption of the gas molecules hinders the movement of the charge carriers between these shorter distances, thus, increasing the resistance with the increase in the concentration of NO_2 gas.

Another aspect observed in the repeatability study is that once the sensor is used, it shows insignificant further change in resistance after being exposed to higher concentration. This could be predicated to the notion of interaction of gas molecules with the active sites, and once these interactions are formed, the changes observed are minimalistic.

IV. CONCLUSION

In the present work, a flexible and disposable NO_2 sensor based on PEDOT:PSS is reported. The sensing layer is developed by drop casting PEDOT:PSS on IDEs structure printed on paper substrate. The successful deposition and surface morphology analysis of the sensing layer are examined using FTIR and SEM, respectively. The gas sensing properties are investigated in sensing range from 0.5 ppm to 50 ppm. The sensor displays substantial % response of 12.97 % at 50 ppm. The response and recovery times, repeatability and reproducibility analysis are also investigated, and the possible sensing mechanisms are presented. Further, a tabular comparative analysis of this work with the background studies is also discussed. The findings of this study demonstrate the sensor's potential for various applications, including healthcare, environmental monitoring, and the automotive industry. However, for such applications analysing the impact of humidity variations on target/ NO_2 sensing performance is crucial and need further experimental studies.

ACKNOWLEDGMENT

This work is supported by the UK Research and Innovation (UKRI) - Engineering and Physical Sciences Research Council (EPSRC) under UKRI Postdoctoral Fellowships Guarantee scheme for Marie Skłodowska-Curie Actions (MSCA) Postdoctoral Fellowship DETECT (EP/X027791/1). This work is also supported with SERB Start-up Grant (SRG/2020/0007111), Department of Science and Technology, India.

REFERENCES

- [1] Y. Lin, L. Huang, L. Chen, J. Zhang, L. Shen, Q. Chen, and W. Shi, "Fully gravure-printed NO_2 gas sensor on a polyimide foil using WO_3 -PEDOT:PSS nanocomposites and Ag electrodes," *Sensors and Actuators B: Chemical*, vol. 216, pp. 176-183, 2015.
- [2] W. Liu, D. Gu, J.-W. Zhang, X.-G. Li, M. N. Rumyantseva, and A. M. Gaskov, "ZnSe/NiO heterostructure-based chemiresistive-type sensors for low-concentration NO_2 detection," *Rare Metals*, vol. 40, no. 6, pp. 1632-1641, 2021.
- [3] Z. Dai, C.-S. Lee, Y. Tian, I.-D. Kim, and J.-H. Lee, "Highly reversible switching from P- to N-type NO_2 sensing in a monolayer Fe_2O_3 inverse opal film and the associated P-N transition phase diagram," *Journal of Materials Chemistry A*, vol. 3, no. 7, pp. 3372-3381, 2015.
- [4] H. K. Gatty, S. Leijonmarck, M. Antelius, G. Stemme, and N. Roxhed, "An amperometric nitric oxide sensor with fast response and ppb-level concentration detection relevant to asthma monitoring," *Sensors and Actuators B: Chemical*, vol. 209, pp. 639-644, 2015.
- [5] K. S. Pasupuleti, M. Reddeppa, D.-J. Nam, N.-H. Bak, K. R. Peta, H. D. Cho, S.-G. Kim, and M.-D. Kim, "Boosting of NO_2 gas sensing performances using GO-PEDOT:PSS nanocomposite chemical interface coated on langasite-based surface acoustic wave sensor," *Sensors and Actuators B: Chemical*, vol. 344, pp. 130267, 2021.
- [6] S. T. Shishiyau, T. S. Shishiyau, and O. I. Lupan, "Sensing characteristics of tin-doped ZnO thin films as NO_2 gas sensor," *Sensors and Actuators B: Chemical*, vol. 107, no. 1, pp. 379-386, 2005.
- [7] R. K. Sonker, S. R. Sabhajeet, S. Singh, and B. C. Yadav, "Synthesis of ZnO nanoparticles and its application as NO_2 gas sensor," *Materials Letters*, vol. 152, pp. 189-191, 2015.
- [8] T. Pham, G. Li, E. Bekyarova, M. E. Itkis, and A. Mulchandani, "MoS₂-Based Optoelectronic Gas Sensor with Sub-parts-per-billion Limit of NO_2 Gas Detection," *ACS Nano*, vol. 13, no. 3, pp. 3196-3205, 2019.
- [9] L. Vigna, A. Verna, S. L. Marasso, M. Sangermano, P. D'Angelo, F. C. Pirri, and M. Cocuzza, "The effects of secondary doping on ink-jet printed PEDOT:PSS gas sensors for VOCs and NO_2 detection," *Sensors and Actuators B: Chemical*, vol. 345, pp. 130381, 2021.
- [10] E. Zampetti, S. Pantalei, A. Muzyczuk, A. Bearzotti, F. De Cesare, C. Spinella, and A. Macagnano, "A high sensitive NO_2 gas sensor based on PEDOT-PSS/TiO₂ nanofibres," *Sensors and Actuators B: Chemical*, vol. 176, pp. 390-398, 2013.
- [11] S.-F. Tseng, Y.-H. Lin, M.-H. Zhou, S.-H. Hsu, and W.-T. Hsiao, "Synthesis of Ti₃C₂T_x/ZnO composites decorated with PEDOT:PSS for NO_2 gas sensors," *The International Journal of Advanced Manufacturing Technology*, vol. 126, no. 5, pp. 2269-2281, 2023.
- [12] M. Chakraborty, J. Kettle, and R. Dahiya, "Electronic Waste Reduction Through Devices and Printed Circuit Boards Designed for Circularity," *IEEE Journal on Flexible Electronics*, vol. 1, no. 1, pp. 4-23, 2022.
- [13] X. Zhang, W. Yang, H. Zhang, M. Xie, and X. Duan, "PEDOT:PSS: From conductive polymers to sensors," *Nanotechnology and Precision Engineering*, vol. 4, no. 4, pp. 045004, 2021.
- [14] Y. Kim, W. Cho, Y. Kim, H. Cho, and J. H. Kim, "Electrical characteristics of heterogeneous polymer layers in PEDOT:PSS films," *Journal of Materials Chemistry C*, vol. 6, no. 33, pp. 8906-8913, 2018.
- [15] A. Beniwal, D. A. John, and R. Dahiya, "PEDOT:PSS-Based Disposable Humidity Sensor for Skin Moisture Monitoring," *IEEE Sensors Letters*, vol. 7, no. 3, pp. 1-4, 2023.
- [16] H. Jiang, W. Wu, Z. Chang, H. Zeng, R. Liang, W. Zhang, W. Zhang, G. Wu, Z. Li, and H. Wang, "In situ polymerization of PEDOT:PSS films based on EMI-TFSI and the analysis of electrochromic performance," vol. 21, no. 1, pp. 722-733, 2021.
- [17] Y. Liu, D. Sun, S. Askari, J. Patel, M. Macias-Montero, S. Mitra, R. Zhang, W.-F. Lin, D. Mariotti, and P. Maguire, "Enhanced Dispersion of TiO₂ Nanoparticles in a TiO₂/PEDOT:PSS Hybrid Nanocomposite via Plasma-Liquid Interactions," *Scientific Reports*, vol. 5, no. 1, pp. 15765, 2015.
- [18] W. Wang, S. Ma, X. Liu, Y. Zhao, H. Li, Y. Li, X. Ning, L. Zhao, and J. Zhuang, " NO_2 gas sensor with excellent performance based on thermally modified nitrogen-hyperdoped silicon," *Sensors and Actuators B: Chemical*, vol. 354, pp. 131193, 2022.
- [19] Y. Seekaew, S. Lokavee, D. Phokharatkul, A. Wisitorsaot, T. Kercharoen, and C. Wongchoosuk, "Low-cost and flexible printed graphene-PEDOT:PSS gas sensor for ammonia detection," *Organic Electronics*, vol. 15, no. 11, pp. 2971-2981, 2014.
- [20] X. Xie, N. Gao, L. Zhu, M. Hunter, S. Chen, and L. Zang, "PEDOT:PSS/PEDOT Film Chemiresistive Sensors for Hydrogen Peroxide Vapor Detection under Ambient Conditions," *Chemosensors*, vol. 11, no. 2: 124, 2023.
- [21] C.-Y. Lin, J.-G. Chen, C.-W. Hu, J. J. Tunney, and K.-C. Ho, "Using a PEDOT:PSS modified electrode for detecting nitric oxide gas," *Sensors and Actuators B: Chemical*, vol. 140, no. 2, pp. 402-406, 2009.